Characterization of Pine Pellet and Peanut Hull Pyrolysis Bio-oils by Negative-Ion Electrospray Ionization Fourier Transform Ion Cyclotron Resonance Mass Spectrometry

ARTICLE *in* ENERGY & FUELS · JUNE 2012

Impact Factor: 2.79 · DOI: 10.1021/ef300385f

6 AUTHORS, INCLUDING:

Amy M. Mckenna
Florida State University
54 PUBLICATIONS **980** CITATIONS
SEE PROFILE

Roger Norris Hilten
University of Georgia
22 PUBLICATIONS **264** CITATIONS
SEE PROFILE

K.C. Das
University of Georgia
131 PUBLICATIONS **3,433** CITATIONS
SEE PROFILE

energy&fuels

Article

pubs.acs.org/EF

Characterization of Pine Pellet and Peanut Hull Pyrolysis Bio-oils by Negative-Ion Electrospray Ionization Fourier Transform Ion Cyclotron Resonance Mass Spectrometry

Jacqueline M. Jarvis,[†] Amy M. McKenna,[‡] Roger N. Hilten,[§] K. C. Das,[§] Ryan P. Rodgers,*[,†,‡] and Alan G. Marshall*[,†,‡]

[†]Department of Chemistry and Biochemistry, Florida State University, 95 Chieftain Way, Tallahassee, Florida 32306, United States

[‡]National High Magnetic Field Laboratory, Florida State University, 1800 East Paul Dirac Drive, Tallahassee, Florida 32310-4005, United States

[§]Driftmier Engineering Center, The University of Georgia, Athens, Georgia 30602, United States

Supporting Information

ABSTRACT: Pyrolysis of solid biomass, in this case pine pellets and peanut hulls, generates a hydrocarbon-rich liquid product (bio-oil) consisting of oily and aqueous phases. Here, each phase is characterized by negative-ion electrospray ionization Fourier transform ion cyclotron resonance mass spectrometry (ESI FT-ICR MS) to yield unique elemental compositions for thousands of compounds. Bio-oils are dominated by O_x species: few oxygens per molecule for the oily phase and many more oxygens per molecules for the aqueous phase. Thus, the increased oxygen content per molecule accounts for its water solubility. Peanut hull bio-oil is much more compositionally complex and contains more nitrogen-containing compounds than pine pellet bio-oil. Bulk C, H, N, O, and S measurements confirm the increased levels of nitrogen-containing species identified in the peanut hull pyrolysis oil by FT-ICR MS. The ability of FT-ICR MS to identify and assign unique elemental compositions to compositionally complex bio-oils based on ultrahigh mass resolution and mass accuracy is demonstrated.

INTRODUCTION

The need for renewable fuels to replace/reduce the current dependence upon petroleum fuels is unavoidable, because fossil fuels are a depletable resource. Political instability, diminishing crude supplies, and undesirable environmental impacts from petroleum combustion provide further incentives. Currently, the development of alternative fuels could lessen the demand for petroleum and potentially replace a significant energy share currently dominated by petroleum-based fuels. Such fuels need to be produced from renewable resources without negatively impacting agricultural industries (land use and irrigation) or competing with current food sources (food versus fuel), as do "generation I" biofuels, such as ethanol.[1,2] In addition, analytical methods for generation III (algae) and IV (advanced) biofuel candidates are forthcoming.[3] Thus, waste and non-foodstuff biomass conversion from "generation II" biofuels, such as plant, forestry, and agricultural residues, as well as municipal wastes and animal byproducts, with continuing supply and low cost, coupled with the ability to generate oils from established farms through low-temperature pyrolysis, make generation II feedstocks an attractive biofuel source.[4,5] Recently, the proof-of-concept has been demonstrated with the establishment of an up to 7 tons/day bio-oil production pilot plant in Finland.[6]

Pyrolysis (i.e., heating in the absence of oxygen) of biomass produces a solid carbon-rich biochar, a liquid hydrocarbon-rich bio-oil, and some low-energy gaseous products. Bio-oil is of interest because of its potential to be upgraded and converted to liquid fuel to replace diesel or gasoline.[5] Bio-oil is a biphasic product with oily (lower) and aqueous (upper) phases; the oil-rich phase may be collected, dried, and processed into useable biofuels.[7] Two main issues in bio-oil production are its high water content and high oxygen content that can create corrosive or unstable bio-oil.[8,9] Conventional petroleum production and refining strategies are not optimized for highly oxygenated materials, because sulfur and nitrogen are the two most abundant heteroatoms in crude oil. As for petroleum crude assays,[10] detailed compositional analysis of pyrolysis biomass products provides insight into the economic feasibility and efficiency of a biomass source targeted for biomass conversion.

Biofuel products vary according to biological source, geographical origin, and processing conditions. For example, the metal content present in pyrolysis products often depends upon the environment in which the feedstock was grown.[11] Biomass comes from the remnants of plant materials and consists of cellulose, hemicellulose, and lignin, whose relative abundances provide one means for characterization. However, the chemical composition of lignin, a major component of wood, is itself poorly characterized.[11,12] The composition of pyrolysis products also heavily depends upon the pyrolysis conditions,[11,13] further complicating characterization.

Prior characterization of biomass and bio-oils has relied on bulk properties (particle size, moisture content, ash content, and elemental C, H, N, and O analyses) and separations based on chemical functionality. As for fossil fuels, such techniques are limited in their ability to predict the optimum biofuel production method and behavior in conversion/upgrading processes, transportation, and storage. Analytical methods for biofuel characterization include gas chromatography−mass

Received: March 2, 2012
Revised: May 11, 2012
Published: May 14, 2012

   dx.doi.org/10.1021/ef300385f | Energy Fuels 2012, 26, 3810−3815

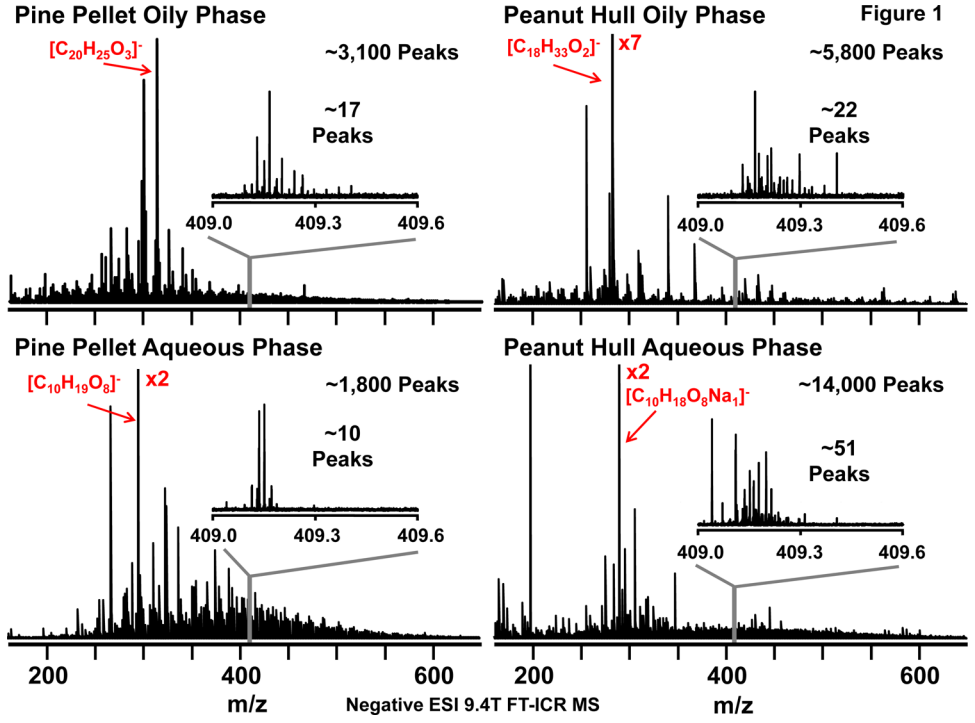

Figure 1. Broadband negative-ion ESI 9.4 T FT-ICR mass spectra of pine pellet oily (top left) and aqueous (bottom left) phases and peanut hull oily (top right) and aqueous (bottom right) phases. Each spectrum is obtained from the sum of 200 co-added time-domain transients and contains ~1800−14 000 peaks above 6 times the baseline root-mean-square (rms) noise with as many as 51 peaks per nominal mass. (Insets) Mass scale-expanded segments, revealing less positive mass defects relative to petroleum-derived materials because of the higher oxygen content (see Figure 4) and greater hydrogen deficiency [Hydrogen deficiency is defined as z in the elemental composition, C_cH_{2c+z}. We prefer to report double bond equivalents (DBE = number of rings plus double bonds to carbon)].

spectrometry (GC−MS), Fourier transform infrared (FTIR) spectroscopy, thermogravimetric analysis (TGA), and others.[14−20] However, highly oxygenated species, characteristic of biomass-related products, are not well-accessed by those techniques because of their polarity, and neither are nonvolatile compounds. Bio-oil compositions have been shown to be extremely complex and obtain a variety of different chemical functionalities, such as ketones, aldehydes, carboxylic acids, alcohols, and phenols.[9,21] Nuclear magnetic resonance (NMR) techniques have been used to probe these functionalities, but the complex nature of the samples makes interpretation difficult and tedious, requiring principal component analyses.[22] Here, we present the detailed characterization of bio-oils by negative-ion electrospray ionization Fourier transform ion cyclotron resonance mass spectrometry (ESI FT-ICR MS[23]), whose ultrahigh mass resolution and mass accuracy enable unique assignment of elemental composition ($C_cH_hN_nO_oS_s$) for thousands of constituents in bio-oils derived from pine and peanut production waste streams.

EXPERIMENTAL SECTION

Sample Preparation. Approximately 2 kg of biomass, either pine or peanut hull pellets, was loaded into a cubical batch reactor with internal dimensions of 20 × 20 cm ($W \times D$). Bio-oils were then produced by heating the reactor containing the feedstock to 500 °C at approximately 8 °C min^{-1} in a furnace. Two ports, an inlet and outlet, both of 1.3 cm outer diameter were used to introduce inert gas flow (N_2 at 1 L min^{-1}) and allow for the escape of product, including inert gas, condensable vapor, and noncondensable product gas (predominantly CO_2 and CO, with additional CH_4, C_2H_6, H_2, and others). The vapor was condensed in a series of stainless-steel traps in an ice bath. Remaining product gas and inert carrier gas were vented to the atmosphere.

Bio-oils generated with the batch system exhibited a two-phase structure with an upper aqueous phase and a lower oily phase. The overall yield of liquid ranged from 60 to 65% (w/w of as-received pellets at 6% moisture content), with approximately 15% (w/w of pellets) in the oily phase. The oily phase was separated from the aqueous fraction via a separatory funnel. Small aliquots (roughly 10 mL) were taken for subsequent mass spectral characterization.

Stock solutions were prepared at a concentration of 1 mg/mL in methanol (HPLC grade, JT Baker, Phillipsburg, NJ, or Sigma-Aldrich, St. Louis, MO). Final samples were further diluted in methanol to 250−500 μg/mL prior to negative-ion ESI FT-ICR MS analysis. Methanol was chosen as a solvent because it completely dissolved the sample and is an optimal ESI solvent. A syringe pump (0.5 μL/min) delivered the samples to the ionization source.

MS. Samples were analyzed with a custom-built 9.4 T FT-ICR mass spectrometer.[24] Data collection was facilitated by a modular ICR data acquisition system (Predator).[25,26] External calibration of the instrument is performed biweekly by use of ESI tuning mix (Agilent, Santa Clara, CA) to correct for temporal drift of the magnetic field. Negative ions generated at atmospheric pressure were introduced into the mass spectrometer via a heated metal capillary. Ions were guided through the skimmer region (~2 Torr) and allowed to accumulate in the first octopole [radio frequency (rf) only].[27] Ions were sent through the quadrupole (mass-transfer mode) to a second octopole, where the ions were collisionally cooled for 1 ms with helium gas (~4−5 × 10^{-6} Torr at gauge) before passage through a transfer octopole to the ICR cell (open cylindrical Penning trap). Octopole ion guides were operated at 2.0 MHz and 240 V_{p-p} rf amplitude.

Multiple (150−200) individual time-domain transients were co-added, Hanning-apodized, zero-filled, and fast Fourier-transformed prior to frequency conversion to the mass-to-charge ratio[28] to obtain the final mass spectrum. The transient length was ~4.6 s. All observed ions were singly charged, as evident from unit m/z spacing between species, which differ by $^{12}C_c$ versus $^{13}C_1{}^{12}C_{c-1}$. Molecular-weight distribution was established with a ThermoFisher LTQ-MS system

dx.doi.org/10.1021/ef300385f | Energy Fuels 2012, 26, 3810−3815

(Thermo Fisher, San Jose, CA) for independent confirmation of the FT-ICR molecular-weight distribution (positive ions) for each bio-oil (see Figure S1 of the Supporting Information).

Data Analysis and Visualization. Data were analyzed and peak lists were generated with custom-built software (MIDAS).[29] Internal calibration of the spectrum was based on a homologous series, whose elemental compositions differ by integer multiples of 14.015 65 Da (i.e., CH_2).[30]

Compounds with the same heteroatom content (i.e., same *n*, *o*, and *s* in $C_cH_hN_nO_oS_s$) but differing in the degree of alkylation may then be grouped together in a spreadsheet.[31] Because a single homologous series does not typically span the entire mass range for a bio-oil sample, multiple homologous series (various O_x species) were needed to achieve broadband internal calibration.

Data are visualized by relative abundance histograms for heteroatom classes greater than 1% relative abundance in either phase (to facilitate direct comparison) and from isoabundance-contoured plots of double bond equivalents (DBE = number of rings plus double bonds to carbon) versus carbon number for members of a single heteroatom class. The abundance scale in isoabundance-contoured plots is scaled relative to the most abundant species in that class.

Elemental Analysis. Bulk elemental analysis was performed with a Thermo Finnigan (San Jose, CA) elemental analyzer (Flash EA 1112) to determine the C, H, N, and S (run 1) and O (run 2) contents in two separate experiments. For C, H, N, and S analyses, 1.5−3 mg of sample was placed in a tin cup, crushed to form a sphere, and placed in the autosampler. All samples were analyzed in quadruplicate, and at least triplicate data were used for calculation of average element percentages. Calibration of the instrument is provided by the analysis of a standard (L-cystine, Thermo, San Jose, CA), and all quadruplicate runs included a separate, independent standard (D,L-methionine, Thermo, San Jose, CA) not used in the initial calibration. A similar procedure was followed for oxygen measurements but with a silver cup.

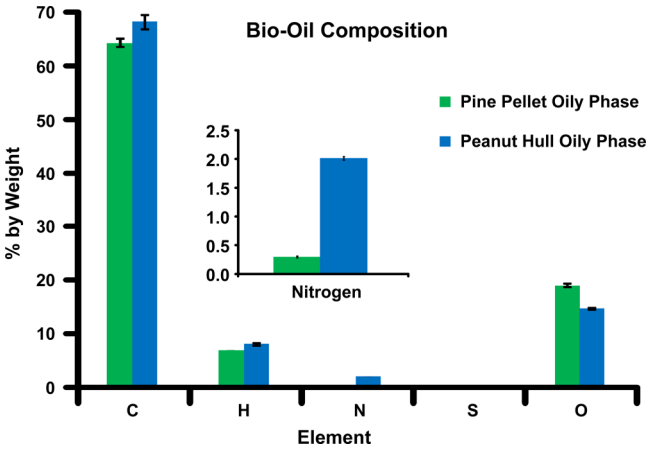

Figure 2. Elemental bulk C, H, N, S, and O elemental analyses from the oily phase of bio-oils collected from the pyrolysis of pine pellets and peanut hull biomass. Error bars are ± the standard deviation. (Inset) Vertical scale-expansion for nitrogen, highlighting the relative abundance of nitrogen for each of the samples.

RESULTS AND DISCUSSION

Elemental Composition Assignment. FT-ICR MS is unparalleled in its ability to simultaneously resolve and identify thousands of peaks in complex natural mixtures at the level of molecular formula assignment.[23,32] The inherent high mass accuracy (100−400 ppb) and ultrahigh resolving power ($m/\Delta m_{50\%}$ = 700 000 at m/z 400, in which $\Delta m_{50\%}$ is mass spectral peak full width at half-maximum peak height) enable unique assignment of elemental composition. To demonstrate the high mass accuracy obtained, a mass accuracy histogram for the peanut hull oily phase components is included in Figure S2 of the Supporting Information. Mass spectral analysis of pine- and peanut-derived bio-oil phases highlights the compositional complexity that limits their characterization by routine analytical techniques. Because pine pellets and pine chips show similar results, only pine pellet data are presented here.

Figure 1 shows broadband negative-ion ESI 9.4 T FT-ICR mass spectra of bio-oils derived from pine pellets and peanut hulls. The pine pellet oily phase is more compositionally

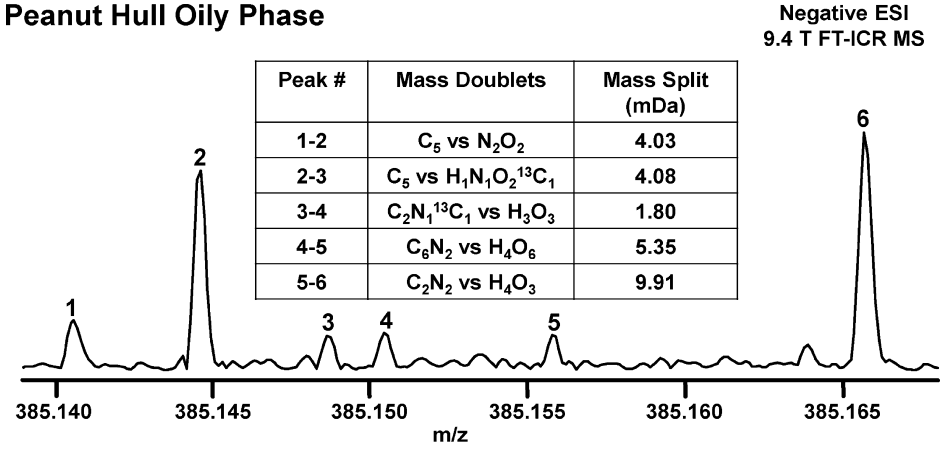

Peak #	Mass Doublets	Mass Split (mDa)
1-2	C_5 vs N_2O_2	4.03
2-3	C_5 vs $H_1N_1O_2{}^{13}C_1$	4.08
3-4	$C_2N_1{}^{13}C_1$ vs H_3O_3	1.80
4-5	C_6N_2 vs H_4O_6	5.35
5-6	C_2N_2 vs H_4O_3	9.91

Peak #	Peak Mass (Da)	Peak Assignment	Mass Error (ppm)
1	385.14061	$C_{20}H_{21}N_2O_6$	0.26
2	385.14461	$C_{25}H_{21}O_4$	0.20
3	385.14870	$C_{20}H_{22}N_1O_6{}^{13}C_1$	0.22
4	385.15047	$C_{18}H_{25}O_9$	0.17
5	385.15584	$C_{24}H_{21}N_2O_3$	0.19
6	385.16574	$C_{22}H_{25}O_6$	0.20

Figure 3. Mass scale-expanded segment, spanning ~30 mDa, of the (−) ESI 9.4 T FT-ICR mass spectrum for the peanut hull oily phase, exposing the inherent compositional complexity of bio-oils. Elemental composition for each of the six above-threshold peaks could be assigned with sub-ppm mass error.

dx.doi.org/10.1021/ef300385f | Energy Fuels 2012, 26, 3810−3815

complex than its aqueous phase [3100 versus 1800 mass spectral peaks with a magnitude greater than 6σ of baseline noise (i.e., the average of three noise values measured at low, intermediate, and high m/z values that span the full molecular-weight distribution)]. However, the pyrolysis products derived from peanut hulls are significantly more compositionally diverse than those from pine pellets. Moreover, the peanut hull aqueous phase is much more complex than its oily phase (14 000 versus 5800 peaks). Note that the most compositionally complex sample (peanut hull aqueous phase) exhibits the least positive mass defects because of more oxygen atoms per molecule.

Bio-oil mass spectra exhibit a lower mass range (~150−800 Da) and less positive mass defects because of higher oxygen content per molecule than conventional petroleum crude oils. The abundance distribution for highly acidic to weakly acidic species in biomass spectra (most notable for the peanut hull oily phase; see the upper right panel of Figure 1) is more asymmetric than for petroleum, because a few highly abundant, highly acidic species dominate the broadband mass spectra.

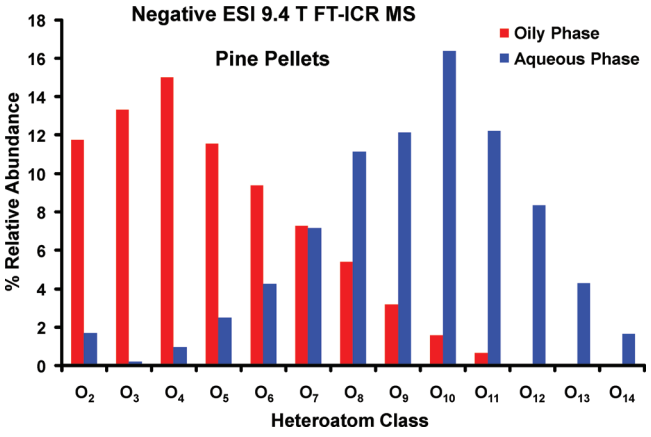

Figure 4. Heteroatom class distribution for the pine pellet oily (red) and aqueous (blue) phases derived from (−) ESI 9.4 T FT-ICR mass spectra. The most abundant class in the oily phase contains 4 oxygens, whereas the most abundant class in the aqueous phase contains 10 oxygens. Only classes with greater than 1% relative abundance in either phase are shown.

For each broadband spectrum, a unique elemental composition ($C_cH_hN_nO_oS_s$) is assigned to each peak with in-house data analysis software.[29] Because little is known about the molecular composition of bio-oil, we performed bulk elemental analysis on the oily phases, to set upper limits on heteroatoms for chemical formula assignment from accurate mass measurements. The results (Figure 2) reveal that the heteroatom content is comprised of mostly oxygen, with very low nitrogen content and no detectable sulfur. The peanut hull oily phase contains significantly more nitrogen and proportionally less oxygen than the pine pellet oily phase.

The complexity of the pyrolysis oil samples can be seen in the 30 mDa mass scale-expanded segment from the (−) ESI 9.4 T FT-ICR mass spectrum of the peanut hull oily phase (Figure 3). The ultrahigh mass resolving power and mass accuracy of FT-ICR MS enable the assignment of elemental composition from sub-parts per million (ppm) mass measurement error for each of six peaks whose magnitude exceeds 6σ of baseline rms noise. The present evidence for five different monoisotopic peaks within 30 mDa invalidates a previous assertion that pyrolysis products are not particularly complex, with monoisotopic peaks separated by no less than 2 Da.[33] The close mass splits between adjacent peaks in Figure 3 clearly demonstrate the need for ultrahigh FT-ICR mass resolution to resolve peaks separated by as little as 1.80 mDa. For example, the minimum mass resolving power, $m/\Delta m_{50\%}$, required to resolve a 1.80 mDa split at 600 Da is 330 000 (for peaks of equal relative abundance). Much higher mass resolving power is

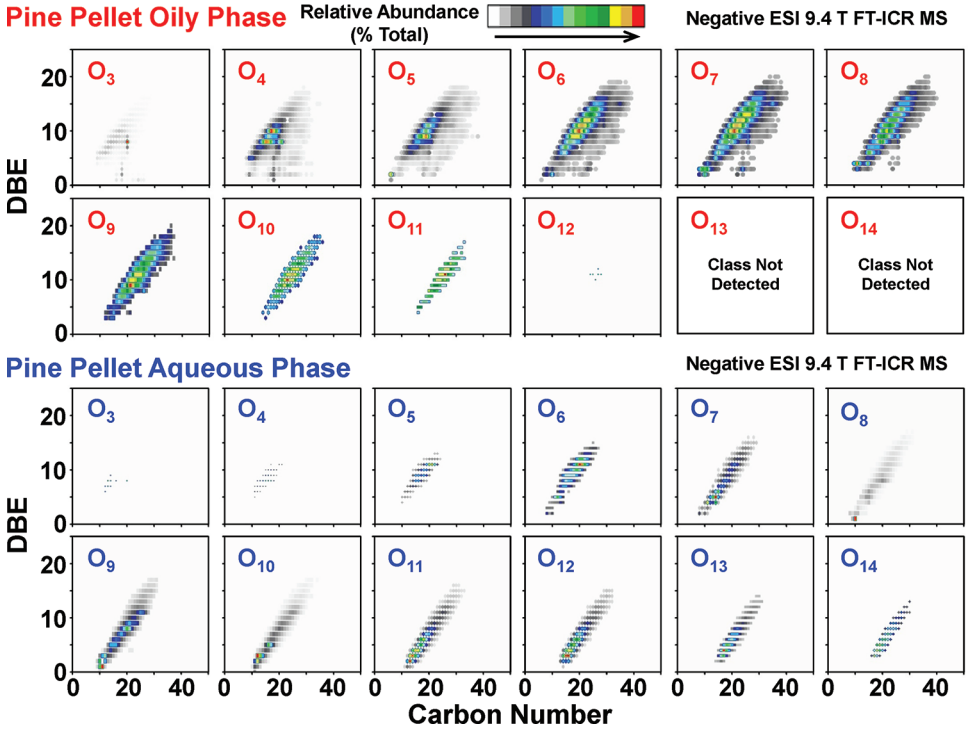

Figure 5. Negative-ion ESI 9.4 T FT-ICR MS isoabundance-contoured plots of DBE versus carbon number for members of the O_3−O_{12} classes in pine pellet oily (top) and pine pellet aqueous (bottom) phases.

dx.doi.org/10.1021/ef300385f | Energy Fuels 2012, 26, 3810−3815

required for peaks of unequal height. In either case, the requisite mass resolving power can be achieved only by FT-ICR MS.

Pine Pellet Bio-oil. Figure 4 shows the heteroatom classes identified at >1% relative abundance in either pine pellet pyrolysis product derived from negative-ion ESI FT-ICR MS. The oily phase is comprised of lower O_x species, with O_4 as the most abundant heteroatom class, whereas the aqueous phase contains a broader range of oxygen atoms per molecule, with O_{10} as the most abundant heteroatom class. Thus, the oxygen content constitutes the fundamental class difference between species in the oily and aqueous phases. The abundant O_2 class compounds correspond to fatty acids and resin acids that are soluble in the oily phase but probably exist as microemulsions in the aqueous phase.

Figure 5 shows pine pellet bio-oil negative-ion ESI isoabundance-contoured plots of DBE versus carbon number for various O_x heteroatom classes. The oxygen classes for both oily and aqueous phases span similar compositional space with slight extension of the pine pellet oily phase to higher carbon number and DBE. Both data sets exhibit a proportionate increase in aromaticity with carbon addition, characteristic of a polymeric structural motif. Isoabundance-contoured plots for the O_2 class are dominated by highly abundant fatty acids and resin acids; thus, little new compositional information is gained by their inclusion. O_2 plots for pine- and peanut-derived bio-oil may be found in Figure S3 of the Supporting Information.

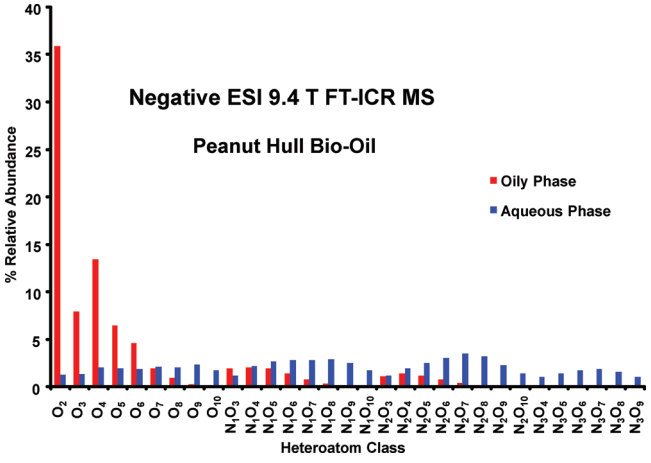

Figure 6. Heteroatom class distribution for peanut hull oily (red) and aqueous (blue) phases derived from (−) ESI 9.4 T FT-ICR mass spectra. The greater compositional complexity of the peanut hull samples relative to pine is evident from the wider range of classes represented.

Peanut Hull Bio-oil. O_x and $N_{1-3}O_x$ heteroatom class distributions for peanut hull oily and aqueous phases from (−) ESI FT-ICR MS (Figure 6) reveal the higher complexity of the peanut hull samples. The oily phase is dominated by O_x species, as for the pine feedstock, but with higher relative abundance of nitrogen-containing compounds. The aqueous phase comprises a diverse collection of O_x and $N_{1-3}O_x$ classes, in accordance with bulk elemental results that revealed a 4-fold higher nitrogen content for the peanut hull materials. Sodium-containing classes are also seen at >1% relative abundance because of the high salt concentration in the bio-oil samples (see Figure S4 of the Supporting Information).

Negative-ion isoabundance-contoured plots of DBE versus carbon number for O_3−O_8, N_1O_3−N_1O_5, and N_2O_3−N_2O_5 classes from peanut hull oily (top) and aqueous (bottom) phases (Figure 7) exhibit multimodal compositional distributions not seen for the pine pellet feedstocks. The multimodal patterns are unique to the oily phase and are seen throughout most of the classes, indicating that they are inherent to the samples and not

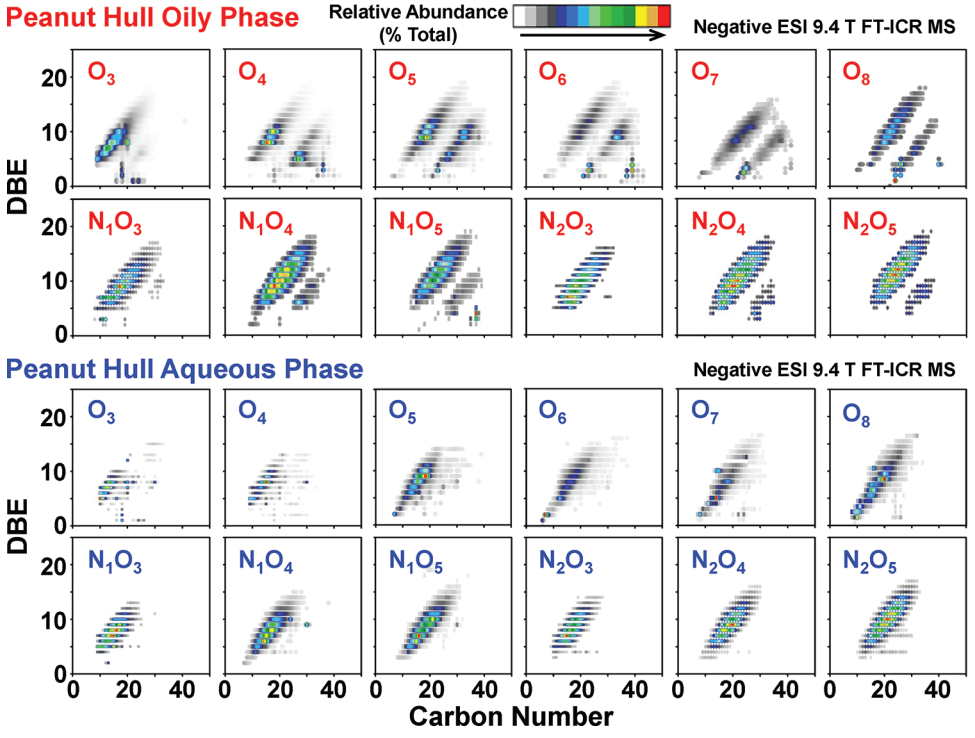

Figure 7. Negative-ion ESI 9.4 T FT-ICR MS isoabundance-contoured DBE versus carbon number plots for members of the O_3−O_7, N_1O_3−N_1O_5, and N_2O_3−N_2O_5 classes from peanut hull oily (top) and aqueous (bottom) phases. Multimodal compositional distributions found for peanut hulls are not observed for the pine pellets.

dx.doi.org/10.1021/ef300385f | *Energy Fuels* 2012, 26, 3810−3815

produced artificially during sample preparation or analysis. In contrast, the compounds that comprise petroleum-derived fuels are known to be a continuum. Thus, the images in Figure 7 demonstrate that biomass pyrolysis oils are compositionally (space and class) distinct from petroleum-derived fuels, for reasons that will be investigated further.

■ CONCLUSION

Here, we present the first detailed characterization of pine pellet and peanut hull bio-oils by negative-ion ESI FT-ICR MS. Unlike petroleum and its products, bio-oils are dominated by O_x species. The compositional complexity of these generation II pyrolysis products is revealed, with several peaks per nominal mass and mass splits as small as 1.80 mDa, requiring ultrahigh-resolution FT-ICR MS for unique elemental composition assignment.

Molecular structure is not determined by mass measurement alone. FTIR spectroscopy conducted by our collaborators has been able to identify some of the structural differences between the pine pellet and peanut hull pyrolysis oils.[8] The O_x species characterized by FT-ICR MS contain a complex mixture of chemical functionalities previously identified by other techniques.[21,22] Future work will focus on the fractionation of bio-oils to enhance characterization of oxygen-containing species.

■ ASSOCIATED CONTENT

Supporting Information

Broadband positive-ion ESI LTQ and 9.4 T FT-ICR mass spectra from the peanut hull oily phase to validate the FT-ICR molecular-weight distribution (Figure S1), mass accuracy histogram for the peanut hull oily phase components observed by (−) ESI 9.4 T FT-ICR MS (Figure S2), negative-ion ESI 9.4 T FT-ICR MS isoabundance-contoured plots of DBE versus carbon number for members of the O_2 class in pine pellet oily and aqueous phases and peanut hull oily and aqueous phases (Figure S3), and heteroatom class distribution for sodium-containing classes of >1% relative abundance in the peanut hull aqueous phase, derived from (−) ESI 9.4 T FT-ICR mass spectra (Figure S4). This material is available free of charge via the Internet at http://pubs.acs.org.

■ AUTHOR INFORMATION

Corresponding Author

*Telephone: +1-850-644-2398 (R.P.R.); +1-850-644-0529 (A.G.M.). Fax: +1-850-644-1366. E-mail: rodgers@magnet.fsu.edu (R.P.R.); marshall@magnet.fsu.edu (A.G.M.).

Notes

The authors declare no competing financial interest.

■ ACKNOWLEDGMENTS

This work was supported by the National Science Foundation (NSF) Division of Materials Research (DMR-06-54118) and the State of Florida. The authors thank Nathan K. Kaiser, John P. Quinn, and Greg T. Blakney for their continued assistance in instrument maintenance, experimental design, and data analysis. The authors also thank Brandie M. Ehrmann for her assistance with data collection, analysis, and interpretation.

■ REFERENCES

(1) Demirbas, A. *Appl. Energy* **2011**, *88*, 17−28.
(2) Tilman, D.; Socolow, R.; Foley, J. A.; Hill, J.; Larson, E.; Lynd, L.; Pacala, S.; Reilly, J.; Searchinger, T.; Somerville, C.; Williams, R. *Science* **2009**, *325*, 270−271.
(3) Wenner, M. *Sci. Am.* **2009**, *March*, 46−51.
(4) Oasmaa, A.; Solantausta, Y.; Arpiainen, V.; Kuoppala, E.; Sipilä, K. *Energy Fuels* **2010**, *24*, 1380−1388.
(5) Czernik, S.; Bridgwater, A. V. *Energy Fuels* **2004**, *18*, 590−598.
(6) Solantausta, Y.; Oasmaa, A.; Sipilä, K.; Lindfors, C.; Lehto, J.; Autio, J.; Jokela, P.; Alin, J.; Heiskanenl, J. *Energy Fuels* **2012**, *26*, 233−240.
(7) Garcia-Perez, M.; Adams, T. T.; Goodrum, J. W.; Geller, D. P.; Das, K. C. *Energy Fuels* **2007**, *21*, 2363−2372.
(8) Hilten, R. N.; Das, K. C. *Fuel* **2010**, *89*, 2741−2749.
(9) Oasmaa, A.; Kuoppala, E.; Gust, S.; Solantausta, Y. *Energy Fuels* **2002**, *17*, 1−12.
(10) Rodgers, R. P.; Schaub, T. M.; Marshall, A. G. *Anal. Chem.* **2005**, *77*, 20A−27A.
(11) Mohan, D.; Pittman, C. U., Jr.; Steele, P. H. *Energy Fuels* **2006**, *20*, 848−889.
(12) Evtuguin, D. V.; Amado, F. M. L. *Macromol. Biosci.* **2003**, *3*, 339−343.
(13) Venderbosch, R. H.; Prins, W. *Biofuels, Bioprod. Biorefin.* **2010**, *4*, 178−208.
(14) Xu, F.; Xu, Y.; Yin, H.; Zhu, X.; Guo, Q. *Energy Fuels* **2009**, *23*, 1775−1777.
(15) Garcia-Perez, M.; Chaala, A.; Pakdel, H.; Kretchmer, D.; Roy, C. *Biomass Bioenergy* **2007**, *31*, 222−242.
(16) Garcia-Perez, M.; Chaala, A.; Pakdel, H.; Kretschmer, D.; Rodrigue, D.; Roy, C. *Energy Fuels* **2006**, *20*, 364−375.
(17) Scholze, B.; Hanser, C.; Meier, D. *J. Anal. Appl. Pyrolysis* **2001**, *58*−*59*, 387−400.
(18) Scholze, B.; Meier, D. *J. Anal. Appl. Pyrolysis* **2001**, *60*, 41−54.
(19) Wang, Y.; Li, X.; Mourant, D.; Gunawan, R.; Zhang, S.; Li, C.-Z. *Energy Fuels* **2011**, *26*, 241−24725.
(20) López, D.; Acelas, N.; Mondragón, F. *Bioresour. Technol.* **2010**, *101*, 2458−2465.
(21) Christensen, E. D.; Chupka, G. M.; Luecke, J.; Smurthwaite, T.; Alleman, T. L.; Iisa, K.; Franz, J. A.; Elliott, D. C.; McCormick, R. L. *Energy Fuels* **2011**, *25*, 5431−5471.
(22) Strahan, G. D.; Mullen, C. A.; Boateng, A. A. *Energy Fuels* **2011**, *25*, 5452−5461.
(23) Marshall, A. G.; Hendrickson, C. L.; Jackson, G. S. *Mass Spectrom. Rev.* **1998**, *17*, 1−35.
(24) Kaiser, N. K.; Quinn, J. P.; Blakney, G. T.; Hendrickson, C. L.; Marshall, A. G. *J. Am. Soc. Mass Spectrom.* **2011**, *22*, 1343−1351.
(25) Blakney, G. T.; Hendrickson, C. L.; Marshall, A. G. *Int. J. Mass Spectrom.* **2011**, 246−252.
(26) Senko, M. W.; Canterbury, J. D.; Guan, S.; Marshall, A. G. *Rapid Commun. Mass Spectrom.* **1996**, *10*, 1839−1844.
(27) Senko, M. W.; Hendrickson, C. L.; Emmett, M. R.; Shi, S. D.-H.; Marshall, A. G. *J. Am. Soc. Mass Spectrom.* **1997**, *8*, 970−976.
(28) Ledford, E. B.; Rempel, D. L.; Gross, M. L. *Anal. Chem.* **1984**, *56*, 2744−2748.
(29) Blakney, G. T.; Robinson, D. E.; Ly, N. V.; Kelleher, N. L.; Hendrickson, C. L.; Marshall, A. G. *Proceedings of the 53rd American Society of Mass Spectrometry Annual Conference on Mass Spectrometry and Allied Topics*; San Antonio, TX, June 5−9, 2005.
(30) Kendrick, E. *Anal. Chem.* **1963**, *35*, 2146−2154.
(31) Hughey, C. A.; Hendrickson, C. L.; Rodgers, R. P.; Marshall, A. G.; Qian, K. *Anal. Chem.* **2001**, *73*, 4676−4681.
(32) Marshall, A. G.; Rodger, R. P. *Proc. Natl. Acad. Sci. U.S.A.* **2008**, *105*, 18090−18095.
(33) Smith, E. A.; Lee, Y. J. *Energy Fuels* **2010**, *24*, 5190−5198.